49th AIAA Aerospace Sciences Meeting including the New Horizons Forum and Aerospace Exposition
4 - 7 January 2011, Orlando, Florida

Interaction of Microvortex Generator Flow with Ramp-Induced Shock/Boundary-Layer Interactions

Adam J. Pierce,* Qin Li,† Yusi Shih† Frank K. Lu,‡ Chaoqun Liu,§
University of Texas at Arlington, Arlington, Texas, 76019

This paper reports the experiments conducted using two different micro vortex generator design on a flat plate with four configuration at Mach 2.5. Configurations include a flat surface (baseline), 5 degree ramp, 25 degree ramp, and a 1 in. diameter cylinder. Surface flow and schlieren were applied experimentally and high-order LES was applied numerically. Results suggest that MVGs have a practical upper limit to their effectiveness on ramp-induced shock/boundary-layer interaction which may be design dependent. The results also suggest the existence of vortex ring production and boundary layer growth due to the effects of micro vortex generators.

I. Introduction

RECENT boundary layer flow control technique is to distribute an array of micro vortex generators (MVGs), whose height is less than the boundary layer thickness, ahead of the region with adverse flow conditions.[1–39] These MVGs are thought to function similarly to conventional vortex generators in energizing the boundary layer via entrainment of the freestream flow by trailing vortices. The main difference between MVGs and conventional vortex generators is that the former is produces less drag. They have apparently been deployed in practice and appear to be beneficial under certain circumstances, such as the low-speed performance of a large transport aircraft[20] and proposed for potential application in supersonic inlets[34] and cabin noise reduction.[1] One form of MVG is wedge shaped as depicted in Fig. 1.

Initial studies were conducted at low speeds and then extended to supersonic flows where the interest lies primarily in reducing or eliminating the separation zone of strong shock/boundary layer interactions. These high-speed studies generally were conducted with an impinging shock due to its relevance in inlets.

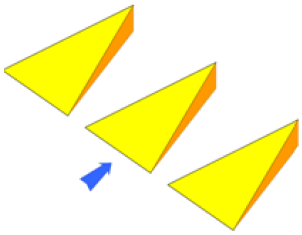

Figure 1. Schematic of an MVG array.

While there is evidence of the benefits of MVGs, the underlying physical mechanisms as to how they affect the boundary layer and especially shock/boundary-layer interactions (SBLIs) remain a topic of ongoing research. It appears that some of the ideas regarding the flow past an MVG are derived from observations of conventional vortex generators at low speeds. Thus, the belief is that the flow past an MVG possesses a horseshoe vortex wrapping around the leading edge of the MVG and trailing off either tip. Horseshoe vortices are expected in boundary layer flows past a three-dimensional object or a protuberance.[40] If the object is bluff, multiple separation zones exist. But for the streamlined MVG protuberance, it is expected that only a single separation zone exists as is evident. Also, it is expected that the horseshoe vortex is weak and has not been properly observed except via the telltale evidence from surface flow visualization.

*Graduate Research Assistant, Aerodynamics Research Center, Department of Mechanical and Aerospace Engineering. Student Member AIAA.
†Visiting Professor, Mathematics Department.
‡Professor and Director, Aerodynamics Research Center, Department of Mechanical and Aerospace Engineering. Associate Fellow AIAA.
§Professor and Director, Center for Numerical Simulation and Modeling, Mathematics Department. Associate Fellow AIAA.

Figure 2 is a schematic of the existing model of the flow past an MVG. Beside the horseshoe vortex, a pair of primary and two pairs of secondary trailing vortices are thought to exist as shown in Fig. 2. Babinsky and co-workers,[24,26,30] from surface flow visualization, and Lee et al.,[37] from large eddy simulations, suggest that a pair of counter-rotating vortices trails downstream of an MVG. The experiments indicate a small separation zone ahead of the compression zone which creates a very small horseshoe vortex on either side of a region devoid of pigment where a herringbone pattern can be seen. This herringbone pattern, as observed in other three-dimensional flows, is thought to be the result of open separation. This open separation zone is dominated by a pair of large, counter-rotating, primary trailing vortices, the direction of which is indicated in Fig. 2.

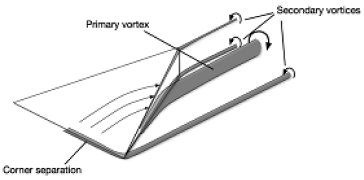

Figure 2. Existing model of multiple trailing vortices shed from an MVG.BabFord.

Babinsky et al.[30] note that the herringbone pattern fades about two MVG lengths downstream. They suggest that this is due to the primary trailing vortices lifting off the surface from their mutual upwash. Other than the primary trailing vortex pair, Babinsky and coworkers found two further pairs of trailing vortices, a pair shed from the top of the MVG and another from the junction between the slant sides of the MVG and the floor. Finally, Babinsky et al.,[30] suggest that there is a small separation around the trailing edge of the ramp although this statement appears incomplete.

Recently, Blinde et al.,[35] through detailed stereoscopic particle image velocimetry, proposed a model shown in Fig. 3. The figure shows hairpin vortices streaming downstream from each MVG. A high-speed region exists between the streaming hairpin vortices. These observations appear to confirm the observation by Babinsky et al. that the primary trailing vortices lift off the surface which, as suggested by Blinde et al., lead to form hairpin vortices.

Most recently, Li and Liu[38,39] using high-order, large eddy simulations, found a complex flowfield arising from the MVG. First, other than the horseshoe vortex, a number of trailing vortices which then suffer a Kelvin–Helmholtz-like breakdown to form vortex rings, which then propagate to a downstream shock/boundary-layer interaction region. This discovery of vortex rings may be considered to be a further refinement of Blinde et al.'s[35] discovery and awaits experimental confirmation.

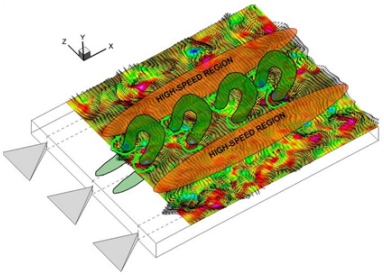

Figure 3. Conceptual sketch of flow downstream of an MVG array, showing the presence of hairpin vortices.

Instead of studying impinging shocks that dominate most of the studies of MVGs, we choose to use compression ramps. There is one overwhelming advantage of using compression ramps for generating the shock instead of impinging the shock from a sharp-edged generator. This is the avoidance of wall effects. The tips on either side of the shock generator produce their own three-dimensional interactions that can grossly distort the flowfield of interest. As a simple rule of thumb, this disturbance can be mapped out by the Mach cone emanating from the tip. Tsumuraya[41] was not successful in isolating the two-dimensional portion of the interaction with fences. On the other hand, there is no possibility of impinging Mach waves into the interaction. Further, the sidewall interaction, while unavoidable, is swept downstream away from the interaction, which helps to minimize their adverse effect.

II. Experiment

A. Facility and Test Hardware

For brevity, only a summary of the experiments are provided with details available in [42]. The experiments were performed in a blowdown wind tunnel at a Mach number of 2.47 ± 0.005. The tunnel operation was controlled by a host computer which opened the control valve to reach steady-state pressure conditions in about 2–3 s.[43] The total pressure was kept at 517 ± 6 kPa (75 ± 0.9 psia). The duration of the flow visualization experiments was less than 10 s long which resulted in a total temperature drop of only about 1–2 K. Thus, despite the blowdown nature of the tunnel, the temperature can be considered to be steady for the present series of experiments. Thus, the unit Reynolds number can also be considered to be steady at 43 million per m.

The test section was 15.2 cm square × 81.28 cm long (6 in.^{2} × 2.67 ft). It was outfitted with extensive optical access from both sides and from the top. A flat plate, 73 cm long (28.75 in), with a sharp leading edge of 15 deg was mounted in the test section[44] over which a boundary layer was developed naturally (Fig. 4). The flat plate was made in layers supported by a sharp tipped rail on each side. The top layer which formed the test surface was made of a number of small, thin plates. These plates butt tightly against each other to form a continuous, flat surface. This modular design allowed for quick configuration changes. A cavity below the top surface allowed pressure tubing, transducer wiring and other elements to be placed. The wiring and tubing were channeled to the rear, either from the side of the test section or from the side of the diffuser, to outside the wind tunnel. A bottom surface encases the cavity.

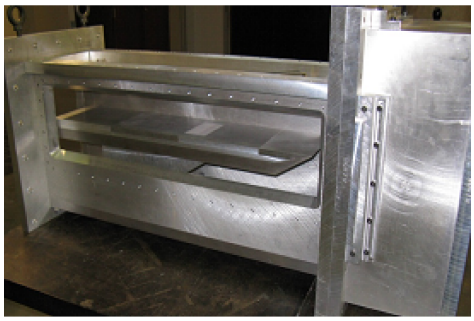

Figure 4. Test section showing flat plate. Flow from right to left.

A microvortex generator (MVG) array was mounted with the leading edge located 272 mm (10.7 in.) downstream of the leading edge of the flat plate. Figure 5 shows the array of five MVGs. Each MVG was 12.95 mm (0.51 in.) long and 1.57 mm (0.062 in.) high. The front of the MVG was 11.7 mm (0.46 in.) wide. The center-to-center spacing between the MVGs was 30.5 mm (1.2 in.). Two styles of MVGs were fabricated based on the designs from [39], with the trailing edge angle of either 45 or 70 deg.

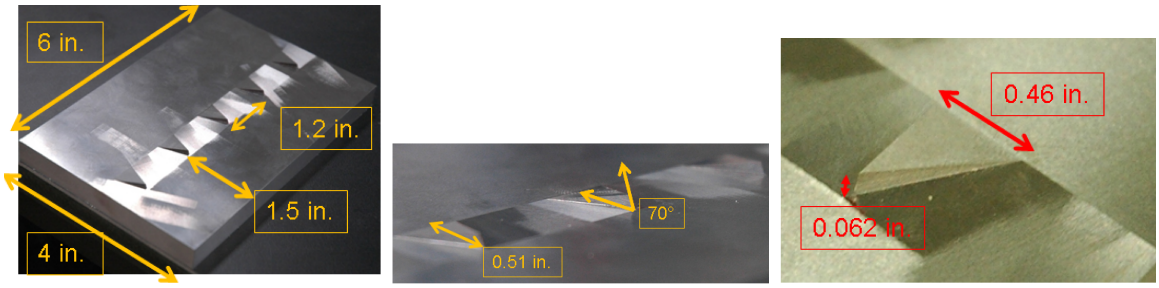

Figure 5. Micro-vortex generator array.

Each MVG style was tested with four plate configurations. The first configuration tested the effects of the MVGs on a simple flat surface. This configuration provide the most simplest case in observing effects on the boundary layer. The second configuration involved the MVGs effect on a 5 degree ramp. For a given Mach number, the strength of the shock generated by the ramp is dependent on the ramp angle. A 5 degree angle ramp at Mach 2.5 produces a wave angle of 27.4° where the density and pressure ratios are 1.26 and 1.38. The shock generated by this ramp is considered to be a weak shock. This configuration is designed to test the sensitivity of the MVG effects when encountering a small disturbance within the boundary layer. The third configuration involved the use of a 25 degree ramp. The oblique shock produced by a 25 degree ramp generates stronger pressure and density ratios of 4.14 and 2.55. This configuration is designed test the stability and strength of the MVGs under more severe conditions. The fourth configuration tested is a 1 in. tall 0.5 in. diameter cylinder. While not considered to be most practical case for supersonic flow, utilizing a cylinder represents the effects produce by a bow shock/boundary–layer interaction. Since the MVGs are a sub–boundary layer design, this configuration would provide information on MVG characteristics and their effectiveness forward of the cylinder where the flow is expected to separate.

B. Diagnostics

Diagnostics that were applied included schlieren video imaging, mean surface pressure measurements down-stream of an MVG and in the bisection of two MVGs, surface flow visualization[45] and laser light sheet visualization using stereo particle image velocimetry hardware and software. The same setup was used to obtain quantitative velocity data. Due to the uniqueness of the last approach, some details are provided here. A schematic of the laser light sheet system is given in Fig. 6. A high-pressure seeding system was installed in the plenum chamber of the wind tunnel to spray calcium carbonate particles (Specialty Minerals

CalEssence 70) with an average diameter of 0.7 μm. It was thought that this is the first time that calcium carbonate has been used for such a purpose.[46] The suitability of calcium carbonate for seeding high-speed aerodynamics flows is discussed in [42].

In addition to seeding the flow from the plenum chamber, local seeding was accomplished by naturally aspirating acetone from a 2.8 mm (0.11 in.) diameter surface pressure tap 138 mm (5.44 in.) upstream along the centerline of an MVG. A flexible tubing connects the pressure tap to a vial of acetone. Since the pressure in the test section is subatmospheric during a run, the acetone is drawn into the boundary layer via the tap. This local lightsheet visualization technique had been used in three-dimensional shock/boundary layer interaction studies.[47,48]

A high-order large eddy simulation was previously reported and is only briefly outlined here.[38,39] The conservation equations were solved in nondimensional form with a fifth-order WENO scheme for the convective terms. Adiabatic, zero normal pressure gradient and no slip conditions were applied on the wall.

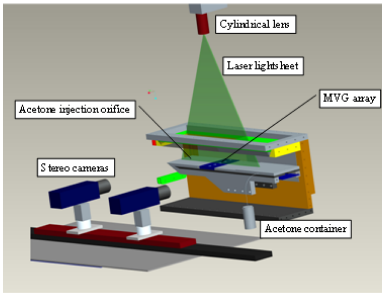

Figure 6. Schematic of laser lightsheet visualization hardware.

C. Governing Equations and Discretization

The governing equations are the non-dimensional Navier-Stokes equations in conservative form written in Cartesian coordinates. A fifth-order WENO scheme was used to discretized the convective terms.[49] A fourth-order central difference scheme was used to discretized the second-order transport terms. Temporal discretization was an explicit, third-order TVD-type Runge-Kutta scheme.[50]

1. Boundary Conditions

Adiabatic, zero normal pressure gradient and non-slip conditions were used on solid surfaces. Only the leading shock from the MVG will reach the upper boundary. This shock is weakened by the expansion waves from the trail-ing edge of the MVG so that no visible reflections are observed. Even if there were reflections, these will exit the domain without impinging on the boundary layer. The outflow boundary conditions were specified as a type of characteristic-based condition which can handle the outgoing flow without reflection.[39] The inflow conditions were generated by first inputting a turbulent mean profile for the streamwise velocity, scaled to the local displacement thickness and the freestream velocity. The pressure in the inflow plane was constant and was the freestream value. The temperature profile was obtained using the Walz equation relating velocity and temperature for an adiabatic wall, with a recovery factor of 0.85.[51] Random fluctuations were added on the primitive variables, i.e., u, v, w, p, ρ. Such inflow conditions are, of course, not the exact solutions of the Navier–Stokes equations. However, the flow solver will adjust and modulate the flow into a weakly turbulent on as it propagates downstream.

2. Code Validation

The code was validated against an asymptotic solution to the Mach 4 flow past a semicircular body. Pressure distributions were oscillation free and the convergence was achieved with a six orders in the decrease of the residuals. The code was also validated by yawing the semicircular body to produce a three-dimensional flow.

3. Grid Generation

Body-fitted grids were used to preserve the geometry and to reduce numerical errors in using the fifth-order WENO scheme. The MVG geometry with a trailing edge inclined at 45 deg. Another MVG configuration, with the same height, had the trailing edge inclined at 70 deg. A total of $n_{span} \times n_{normal} \times n_{stream} = 128 \times 192 \times 1\,600 = 32\,321\,000$ grids were used. Details of grid generation can be found in [39].

III. Results and Discussion

The results of the flat plate configuration is shown in Fig. 7 where several known MVG characteristics are revealed. Flow direction is from left to right. The most noticeable are the two lines trailing from the

center of the MVG. Figure 7 shows that this feature, previously associated with a pair of counter-rotating vortices[30] presists several MVG lengths downstream. Leading edge separation and horseshoe shape flow are also clearly visible on all three MVG locations. The line perpendicular to the flow in Fig. 7 is the location where two plates are joined. This location is also the leading edge of the 5 and 25 degree ramps.

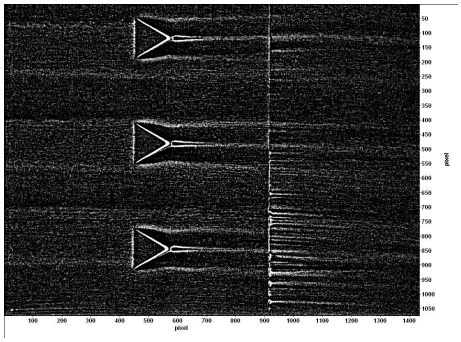

Figure 7. Processed image of MVG45 flat plate configuration.

Figure 8 depicts the results of the images collected by the PIV system with and without vortex generators for a flat surface. The increase in the boundary layer height due to the MVGs is clearly visible. Two possible conclusions can be obtained from the images. The vortices being generated are either lifting off the surface as described by Babinsky et al. or vortex rings are being generated and growing in size as described by Li and Liu[38]. Comparing experimental and LES results which include Fig. 8(c) would support the conclusion that vortex rings are being generated and grow in size. It must be mentioned that the MVG design tested here are different from those tested by Babinsky. Three-dimensional verification of vortex ring structures could not be confirmed experimentally, at present however, two dimensional results of schlieren and surface flow visualization agree well with LES.

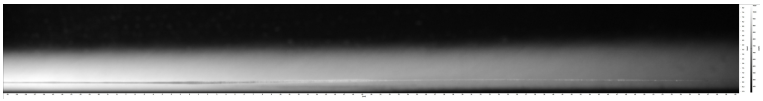

(a) Bare flat plate.

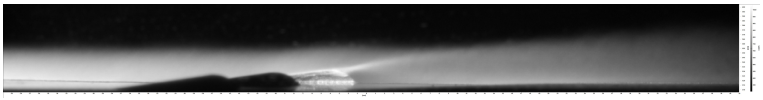

(b) MVG present time-averaged.

(c) MVG present; instantaneous

Figure 8. Laser lightsheet visualizations.

The 5 degree ramp with either of the two MVG configurations yielded similiar results to the flat plate. The existence of a weak shock as previously stated was verified in the schlieren imagery. Fig. 9(a) also verifies the height of the MVG is approximately half the boundary layer thickness. Downstream of the MVG it appears that the boundary layer grows to 1.5 times the boundary layer height. This image clearly shows that density gradients are occurring within this extended boundary layer and are a direct result of the

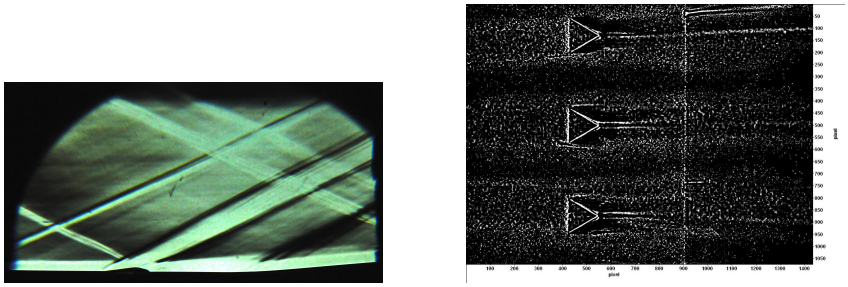

(a) Schlieren (b) Processed Image

Figure 9. Results for MVG45 with 5 degree ramp .

MVGs. PIV data also confirms the increase in boundary layer effects with an approximate increase from 4 mm to 8 mm [42]. As the effects of the MVG translates through the weak shock generated by the ramp, it is reasonable to conclude that the structure and strength of the generated vortex survives the pressure and density gradients created by the weak 5 degree ramp. Confirmation is also shown in Fig. 9(b) where surface features due to the vortices are still visible downstream of the ramps leading edge. In Fig. 9(a), the incoming shock located at the MVG was determined to be near the side wall of the test section and does not impact the MVG itself.

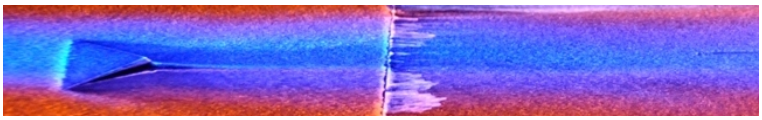

Figure 10. View of MVG45 with 5 degree ramp configuration.

Figure 10 reveals one MVG characteristic that is worth noting. The pinkish color in the image indicates mixing of surface flow paints fluorescent blue and fluorescent orange. This mixed color can be seen traveling from the tip of the MVGs leading edge to the trailing MVG center and continues downstream to approximately 4 to 5 MVG lengths. At least from surface indications, the flow past the MVG appears constrained and does not spread. This constraint may be due to the horseshoe vortex.

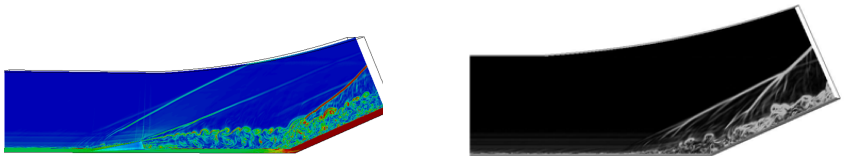

(a) With MVG70 (b) Without MVG

Figure 11. Numerical schlieren results for 25 degree ramp.

For the more severe 25 degree case, LES yield similar results to the 5 degree ramp. Numerical schlieren results are shown in Fig. 11. The analysis by Li and Liu[38] shows that ring vorticies disrupted by the shock but were not totally destroyed. the generation of vortex flow from the MVG will in fact survive pressure and density gradient produced by a 25 degree ramp configuration. The ability to survive stronger pressure and density gradients may indicated that vortices and vortex rings being generated are strongly resistant to change.

It is well known that the shock system of a separated shock/boundary-layer interaction exhibits a lambda foot structure, with the leading shock, also called the separation shock, inclined gently to impinge the boundary layer near the upstream influence. Such a well-organized wave system has been studied experimentally,

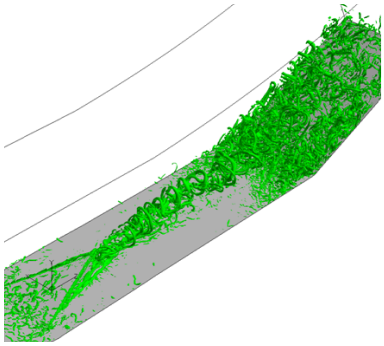

Figure 12. 3D LES flow revealing vortex ring structure.

numerically and analytically and there is good understanding of the mutual interaction between the boundary layer and the shock wave via the free interaction concept[52] and via triple deck theory.[53] This can be seen in Fig. 13(a). However, the wake of the MVG destroys all notion of a well-understood interaction. For example, Fig. 13(a) shows the destruction of the distinct separation shock. This can also be seen in the numerical schlieren images presented in Fig. 11. The three-dimensional nature of the interaction of the MVG wake with the separated shock/boundary-layer interaction is evident in Fig. 12 which plots the λ_2 iso-surface, used as an indicator of vortices.

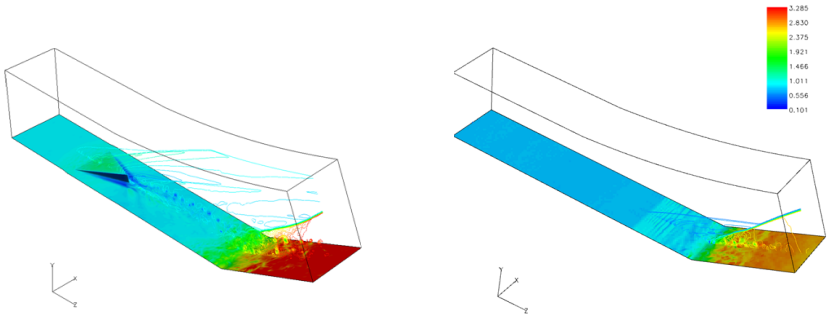

(a) With MVG70 (b) Without MVG

Figure 13. LES pressure results for 25 degree ramp.

Unfortunately the experimental test conducted using a 25 degree ramp configuration were unsuccessful and therefor the LES results could not be verified experimentally. However, results of the surface flow and schlieren test for the other configuration have been performed and reported in reference [42] which would suggest high confidence in LES results. The test performed on a 25 degree ramp does provides an opportunity to examine the effects of MVGs on the most extreme case, that being an unstart condition. Fig. 14 show the results for the the test conducted with and without MVG for this case. As seen in the figures, it is apparent that there is an upper limit on the effectiveness of MVGs. While capable of surviving strong pressure and density gradients at Mach 2.5, it is clearly evident that the pressure and density gradients encountered during an unstart condition are too strong for the vortices to have any major effect. The resulting test performed do show that the vortices being generated will have have some effect on the separation itself. This is indicated when comparing the the shape of the separated region along the of the leading edge of the 25 degree ramp with and without MVGs. The vortices being generated by the MVGs appear stable. This is indicated by the MVG flow pattern in Fig. 14(a) where the MVG effects can be traced up to the edge of separation. Upon reaching the separated region the vortices generated are turned toward the outer edge of the plate.

The final configuration involves the effects of the MVGs on a 1 in.upright diameter cylinder. The results of the surface flow test in Fig. 15 clearly show that the outer two vortices created by the MVGs are diverted around the cylinder. This would suggest that the placement of the MVG is important when considering

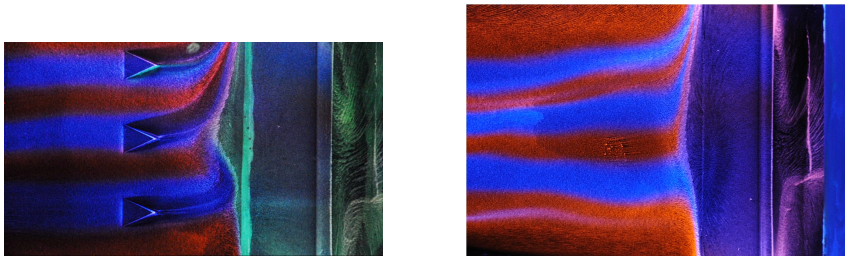

(a) With MVG45 (b) Without MVGs

Figure 14. Experimental surface flow results of the unstart condition.

bow shock/boundary layer interactions. In order to have a positive effect the results suggest that the MVGs may need to be positioned perpendicular to the disturbance. However the strength of the vortex is an important aspect when considering this condition. Being approximately near the stagnation point of the bow shock/boundary–layer interaction, the center vortex appears to vanish near the disturbance. The surface flow results shows that vortices were generated and continue up to the location of the disturbance where the flow has separated. Upon intersecting with the disturbance it appears that the vortex no longer exist, however a conclusion could not be confirmed from the image alone and schlieren and PIV test were not performed for this configuration. Similar to the unstart conditions, the vortices produced by the MVGs were unable to penetrate the bow shock/boundary layer interaction condition further suggesting a limit to the effectiveness of the MVGs. The results may also suggest that this upper limit may be dependent on MVG design.

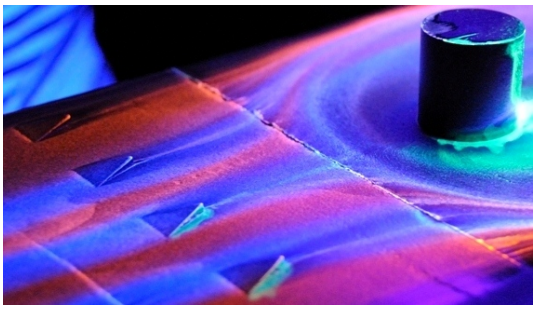

Figure 15. Experimental surface flow results of MVG on cylinder.

IV. Conclusions

The tests performed here involved two MVG designs under four different plate configuration. The first configuration showed the basic characteristics of MVGs and how they effect the boundary layer. Test conditions and data collected were accomplished and verified using images collected from PIV, schlieren and surface flow techniques. The results showed that the effects produced by the MVGs increased the boundary layer thickness approximately 1.5 times. The schlieren images confirmed the boundary layer growth as well as verified the existence of density gradients occurring downstream of the MVGs. The 5 degree ramp yielded similar results to the flat plate configuration. The vortex strength and structure was shown to survive the weak pressure and density gradient generated by an oblique shock. For the more severe 25 degree case, LES analysis concluded that the strength and structure of the vortex rings generated will also survive as well as disrupted the lambda shock structure within the boundary layer. While not able to be confirmed the LES results experimentally, the 25 degree ramp test provided MVG characteristics in the most extreme case. The results suggests that there is an upper limit as to the effectiveness of the MVGs on boundary layer conditions. The final case involved a cylinder where bow shock/sub-boundary layer was tested. Results concluded that

MVGs are sensitive to extreme pressure and density gradients as well as further supporting the upper limit effectiveness. This upper limit effectiveness may be dependent on MVG design.

Acknowledgments

The authors gratefully acknowledge funding for this work via AFOSR Grant No. FA9550-08-1-0201 monitored by Dr. John Schmisseur. The authors thank the assistance of Rod Duke, Yusi Shih and David Whaley with the experiments. David Whaley was supported by a High School Research Internship under a Texas Youth in Technology grant from the Texas Workforce Commission, administered by Dr. J. Carter M. Tiernan.

References

[1]Holmes, A. E., Hickey, P. K., Murphy, W. R., and Hilton, D. A., "The Application of Sub-Boundary Layer Vortex Generators to Reduce Canopy 'Mach Rumble' Interior Noise on the Gulfstream III," AIAA Paper 1987–0084, 1987.

[2]Lin, J. C., McGhee, S. K., and Valarezo, W. O., "Separation Control on High-Lift Airfoils via Micro-Vortex Generators," *Journal of Aircraft*, Vol. 31, No. 6, 1994, pp. 1317–1323.

[3]Lin, J. C., "Control of Turbulent Boundary-Layer Separation Using Micro-Vortex Generators," AIAA Paper 1999-3404, 1999.

[4]Ashill, P. R., Fulker, J. L., and Hackett, K. C., "Research at DERA on Sub Boundary Layer Vortex Generators (SBVGs)," AIAA Paper 2001–0887, 2001.

[5]Allan, B. G., Yao, C.-S., and Lin, J. C., "Numerical Simulations of Vortex Generator Vanes and Jets on a Flat Plate," AIAA Paper 2002–3160, 2002.

[6]Ashill, P. R., Fulker, J. L., and Hackett, K. C., "Studies of Flows Induced by Sub Boundary Layer Vortex Generators (SBVGs)," AIAA Paper 2002–0968, 2002.

[7]Jenkins, L. N., Gorton, S. A., and Anders, S. G., "Flow Control Device Evaluation for an Internal Flow with an Adverse Pressure Gradient," AIAA Paper 2002–0266, 2002.

[8]Lin, J. C., "Review of Research on Low-Profile Vortex Generators to Control Boundary-Layer Separation," *Progress in Aerospace Sciences*, Vol. 38, No. 4–5, 2002, pp. 389–420.

[9]Patel, M. P., Carver, R., Lisy, F., Prince, T. S., and Ng, T., "Detection and Control of Flow Separation Using Pressure Sensors and Micro-Vortex Generators," AIAA Paper 2002–0268, 2002.

[10]Patel, M. P., Prince, T. S., Carver, R., DiCocco, J. M., Lisy, F. J., and Ng, T. T., "Deployable Flow Effectors for Phantom Yaw Control of Missiles at High Alpha," AIAA Paper 2002–2827, 2002.

[11]Patel, M. P., Prince, T. S., Carver, R., DiCocco, J. M., Lisy, F. J., and Ng, T. T., "Control of Aircraft Stall via Embedded Pressure Sensors and Deployable Flow Effectors," AIAA Paper 2002–3170, 2002.

[12]Rae, A. J., Galpin, S. A., and Fulker, J., "Investigation into Scale Effects on the Performance of Sub Boundary-Layer Vortex Generators on Civil Aircraft High-Lift Devices," AIAA Paper 2002–3274, 2002.

[13]Tai, T. C., "Effect of Midwing Vortex Generators on V-22 Aircraft Forward-Flight Aerodynamics," *Journal of Aircraft*, Vol. 40, No. 4, 2003, pp. 623–623.

[14]Jirásek, A., "A Vortex Generator Model and its Application to Flow Control," AIAA Paper 2004–4965, 2004.

[15]Osborn, R. F., Kota, S., Hetrick, J. A., Geister, D. E., Tilmann, C. P., and Joo, J., "Active Flow Control Using High-Frequency Compliant Structures," *Journal of Aircraft*, Vol. 41, No. 3, 2004, pp. 603–609.

[16]Wik, E. and Shaw, S. T., "Numerical Simulation of Micro Vortex Generators," AIAA Paper 2004–2697, 2004.

[17]Ahmad, K. A., McEwan, W. T., Watterson, J. K., and Cole, J. S., "Numerical Study of a Vibrating Sub-Boundary Layer Vortex Generator," AIAA Paper 2005–4648, 2005.

[18]Ahmad, K. A., McEwan, W. T., Cole, J. S., and Briggs, I., "Sub-Boundary Layer Vortex Generator Control of a Separated Diffuser Flow," AIAA Paper 2005–4650, 2005.

[19]Jirásek, A., "Vortex-Generator Model and Its Application to Flow Control," *Journal of Aircraft*, Vol. 42, No. 6, 2005, pp. 1486–1491.

[20]Bohannon, K. S., "Passive Flow Control on Civil Aircraft Flaps Using Sub-Boundary Layer Vortex Generators in the AWIATOR Programme," AIAA Paper 2006–2858, 2006.

[21]Jirásek, A., "Development and Application of Design Strategy for Design of Vortex Generator Flow Control in Inlets," AIAA Paper 2006–1050, 2006.

[22]Anderson, B. H., Tinapple, J., and Sorber, L., "Optimal Control of Shock Wave Turbulent Boundary Layer Interactions Using Micro-Array Actuation," AIAA Paper 2006–3197, 2006.

[23]Babinsky, H., Makinson, N. J., and Morgan, C. E., "Micro-Vortex Generator Flow Control for Supersonic Engine Inlets," AIAA Paper 2007–2007, 2007.

[24]Holden, H. and Babinsky, H., "Effect of Microvortex Generators on Separate Normal Shock/Boundary Layer Interactions," *Journal of Aircraft*, Vol. 44, No. 1, 2007, pp. 89–96.

[25]Shinn, A. F., Vanka, S. P., Mani, M., Dorgan, A., and Michal, T., "Application of BCFD Unstructured Grid Solver to Simulation of Micro-Ramp Control of Shock/Boundary Layer Interactions," AIAA Paper 2007–3914, 2007.

[26]Babinsky, H. and Ogawa, H., "SBLI Control for Wings and Inlets," *Shock Waves*, Vol. 18, No. 2, 2008, pp. 89–96.

[27]Ghosh, S., Choi, J.-I., and Edwards, J. R., "RANS and Hybrid LES/RANS Simulation of the Effects of Micro Vortex Gener-tors Using Immersed Boundary Methods," AIAA Paper 2008–3728, 2008.

[28]Meunier, M. and Brunet, V., "High-Lift Devices Performance Enhancement Using Mechanical and Air-Jet Vortex Generators," *Journal of Aircraft*, Vol. 45, No. 6, 2008, pp. 2049–2061.

[29]Anderson, B. H., Mace, J. L., and Mani, M., "Active 'Fail Safe' Micro-Array Flow Control For Advanced Embedded Propulsion Systems," AIAA Paper 2009–0920, 2009.

[30]Babinsky, H., Li, Y., and Pitt Ford, C. W., "Microramp Control of Supersonic Oblique Shock-Wave/Boundary-Layer Interactions," *AIAA Journal*, Vol. 47, No. 3, 2009, pp. 668–675.

[31]Domel, N. D., Baruzzini, D., and Miller, D. N., "CFD Results for Shock-Boundary Layer Flow Control with Micro-Ramps at Various Grid Densities," AIAA Paper 2009–4016, 2009.

[32]Galbraith, M. C., Orkwis, P. D., and Benek, J. A., "Multi-Row Micro-Ramp Actuators for Shock Wave Boundary-Layer In-teraction Control," AIAA Paper 2009–0321, 2009.

[33]Lee, S., Loth, E., Georgiadis, N. J., and DeBonis, J. R., "Effect of Mach Number on Flow Past Micro-Ramps," AIAA Paper 2009–4181, 2009.

[34]Rybalko, M., Loth, E., Chima, R. V., Hirt, S. M., and DeBonis, J. R., "Micro-Ramps for External Compression Low-Boom Inlets," AIAA Paper 2009–4206, 2009.

[35]Blinde, P. L., Humble, R. A., van Oudheusden, B. W., and Scarano, F., "Effects of Micro-Ramps on a Shock Wave/Turbulent Boundary Layer Interaction," *Shock Waves*, Vol. 19, No. 6, 2009, pp. 507–520.

[36]Bur, R., Coponet, D., and Carpels, Y., "Separation Control by Vortex Generator Devices in a Transonic Channel Flow," *Shock Waves*, Vol. 19, No. 6, 2009, pp. 521–530.

[37]Lee, S., Goettke, M. K., Loth, E., Tinapple, J., and Benek, J., "Microramps Upstream of an Oblique-Shock/Boundary-Layer Interaction," *AIAA Journal*, Vol. 48, No. 1, 2010, pp. 104–118.

[38]Li, Q. and Liu, C., "LES for Supersonic Ramp Control Flow Using MVG at $M = 2.5$ and $Re_\theta = 1440$," AIAA Paper 2010–0592, 2010.

[39]Li, Q. and Liu, C., "Numerical Investigation on the Effects of the Declining Angle of the Trailing Edge of MVG," AIAA Paper 2010–0714, 2010.

[40]Sedney, R., "A Survey of the Effects of Small Protuberances on Boundary-Layer Flows," *AIAA Journal*, Vol. 11, No. 6, 1973, pp. 782–792.

[41]Tsumuraya, M., *An Experimental Study of Incident Shock Wave/Turbulent Boundary Layer Interactions*, MS thesis, Princeton University, 1981.

[42]Pierce, A. J., *Experimental Study of Micro-Vortex Generators at Mach 2.5*, MSAE thesis, University of Texas at Arlington, 2010.

[43]Braun, E. M., Lu, F. K., Mitchell, R. R., Wilson, D. R., and Dutton, J. C., "Supersonic Blowdown Wind Tunnel Control Using LabVIEW," AIAA Paper 2008–0852, 2008.

[44]Mitchell, R. R. and Lu, F. K., "Development of a Supersonic Aerodynamic Test Section using Computational Modeling," AIAA Paper 2009–3573, 2009.

[45]Pierce, A. J., Lu, F. K., Bryant, D. S., and Shih, Y., "New Developments in Surface Oil Flow Visualization," AIAA Paper 2010–4353, 2010.

[46]Raffel, M., Willert, C., Wereley, S., and Kompenhans, J., *Particle Image Velocimetry: A Practical Guide*, Springer, Berlin, 2nd ed., 2007.

[47]Settles, G. S. and Lu, F. K., "Conical Similarity of Shock/Boundary-Layer Interactions Generated by Swept and Unswept Fins," *AIAA Journal*, Vol. 23, No. 7, 1985, pp. 1021–1027.

[48]Settles, G. S., "Modern Developments in Flow Visualization," *AIAA Journal*, Vol. 24, No. 8, 1986, pp. 1313–1323.

[49]Jiang, G.-S. and Shu, C.-W., "Efficient Implementation of Weighted ENO Schemes," *Journal of Computational Physics*, Vol. 126, No. 1, 1996, pp. 202–228.

[50]Cockburn, B. and Shu, C.-W., "TVB Runge–Kutta Local Projection Discontinuous Galerkin Finite Element Method for Conservation Laws II: General Framework," *Mathematics of Computation*, Vol. 52, No. 186, 1989, pp. 411–443.

[51]Walz, A., "Compressible Turbulent Boundary Layers," *The Mechanics of Turbulence: Proceedings of Colloque Internationale sur La Mechanique de la Turbulence, Marseille, August 28 to September 2, 1961*, Science Publishers, Inc., New York, 1964.

[52]Chapman, D. R., Kuehn, D. M., and Larson, H. K., "Investigation of Separated Flows in Supersonic and Subsonic Streams with Emphasis on the Effect of Transition," NACA-TR-1356, 1958.

[53]Adamson, T. C. and Messiter,Jr., A. F., "Analysis of Two-Dimensional Interactions Between Shock Waves and Boundary Layers," *Annual Review of Fluid Mechanics*, Vol. 12, 1980, pp. 103–138.